

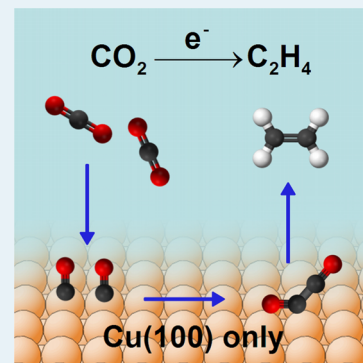
# Structure Sensitivity of the Electrochemical Reduction of Carbon Monoxide on Copper Single Crystals

Klaas Jan P. Schouten, Elena Pérez Gallent, and Marc T. M. Koper\*

Leiden Institute of Chemistry, Leiden University, Einsteinweg 55, PO Box 9502, 2300 RA, Leiden, The Netherlands

**ABSTRACT:** The product selectivity in the electrochemical reduction of carbon dioxide and carbon monoxide strongly depends on the atomic configuration of the copper electrode surface. On Cu(111), methane formation is favored, whereas on Cu(100), ethylene formation is favored, with selective ethylene formation at low overpotentials. To distinguish the reactivity of (100) terraces vs (100) steps, we have studied carbon monoxide reduction on Cu(322), with the  $[5(111) \times (100)]$  orientation, and Cu(911), with the  $[5(100) \times (111)]$  orientation. Only on Cu(911) is the selective ethylene formation at low overpotentials observed, indicating that this reaction pathway occurs only on (100) terraces. We also show that the reduction of ethylene oxide to ethylene is significantly faster on Cu(100) compared with Cu(111), giving further evidence to the importance of the associated intermediate for ethylene formation. On Cu(110), the potential dependence of methane and ethylene formation is similar to Cu(111), and we have observed a primary alcohol among the products.

**KEYWORDS:** carbon monoxide, carbon dioxide, copper electrodes, single crystals, structure sensitivity, Cu(100), ethylene



## 1. INTRODUCTION

The electrochemical reduction of carbon dioxide to hydrocarbons has been the subject of various investigations, since  $\text{CO}_2$  is a vast and sustainable carbon feedstock and the conversion of  $\text{CO}_2$  to hydrocarbons could mitigate the increasing  $\text{CO}_2$  emissions.<sup>1,2</sup> In 1985, it was discovered by Hori et al. that on copper electrodes, carbon dioxide can be electrochemically reduced to hydrocarbons, mainly methane and ethylene.<sup>3</sup> Especially the formation of ethylene, which is widely used in the chemical industry, is unique and takes place to a significant extent only on copper electrodes. Since its discovery, this reaction has been studied extensively. On single crystal copper electrodes, the selectivity toward hydrocarbons as well as the ratio of methane over ethylene have been shown to depend on the atomic configuration of the electrode surface.<sup>2,4–6</sup> Hori et al. have shown that ethylene formation is favored on Cu(100) surfaces and that the presence of small amounts of (111) and (110) steps in the (100) terraces increases the selectivity to ethylene further.<sup>4</sup> Methane formation, on the other hand, is favored on Cu(111) terraces. Carbon monoxide is a well-known intermediate in the reduction of  $\text{CO}_2$ ,<sup>2,7,8</sup> and the reduction of  $\text{CO}_2$  and CO have the same dependence on the atomic surface structure.<sup>9</sup>

Recently, we have shown that for CO reduction, ethylene can be formed via two different pathways: (1) on Cu(100), CO is reduced to only ethylene and not methane at relatively low overpotentials, presumably through the formation of a surface adsorbed CO dimer; and (2) on both Cu(100) and Cu(111), at higher overpotentials, CO is reduced to methane and ethylene simultaneously, suggesting a shared intermediate.<sup>5</sup> To investigate whether this selective ethylene formation on Cu(100) at low overpotentials is sensitive toward (100) terraces or (100)

step sites, we report here on the electrochemical reduction of CO on two stepped Cu single crystals: Cu(322), with the  $[5(111) \times (100)]$  orientation, and Cu(911), with the  $[5(100) \times (111)]$  orientation. We have investigated the reactivity of these surfaces using online electrochemical mass spectrometry (OLEMS).<sup>10</sup> This tip-based sampling technique allows following the formation of volatile reaction intermediates and products while changing the potential at the electrode surface.

## 2. EXPERIMENTAL SECTION

**2.1. Electrochemistry.** All experiments were carried out in an electrochemical cell using a three-electrode assembly at room temperature. The cell and glassware were boiled in ultraclean water (Millipore Milli-Q gradient A10 system, 18.2  $\text{M}\Omega\cdot\text{cm}$ ) before each experiment. A gold wire was used as the counter electrode, and a reversible hydrogen electrode (RHE) in the same electrolyte was used as the reference electrode. All potentials in this paper are referred to this electrode. The potential was controlled using an Ivium A06075 potentiostat.

The single crystal copper electrodes used were bead-type electrodes (icryst) cut and polished with an accuracy down to 0.5°. Prior to each experiment, the electrode was electro-polished in 66%  $\text{H}_3\text{PO}_4$  at 3 V vs a Cu counter electrode for 10 s.<sup>11</sup> After polishing, the surface quality was verified regularly using blank voltammetry in 0.1 M NaOH.<sup>12</sup>

The experiments were carried out in 0.1 M  $\text{K}_2\text{HPO}_4$  + 0.1 M  $\text{KH}_2\text{PO}_4$  (pH 7) prepared from high-purity reagents (Sigma-Aldrich TraceSelect) and ultraclean water. Argon (Air Products,

Received: March 28, 2013

Revised: May 3, 2013

Published: May 8, 2013

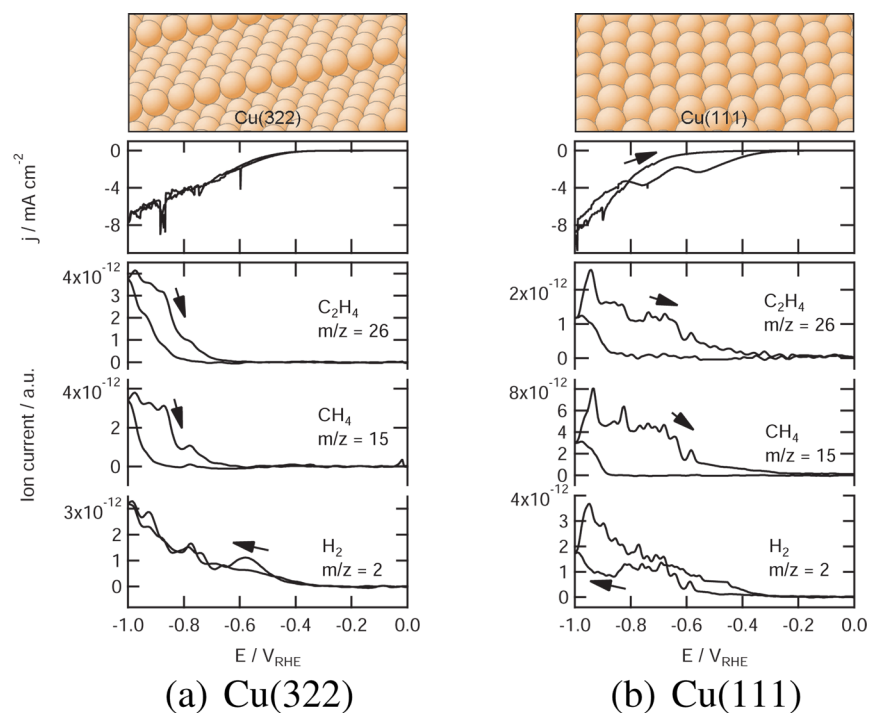


**Figure 1.** The reduction of CO in a saturated ( $\sim 1$  mM) phosphate buffer (pH 7) on Cu(322) (a) and Cu(111) (b). The top panels show the crystal facets; the middle panels, the corresponding cyclic voltammograms; and the bottom panels, the associated mass fragments of volatile products measured with OLEMS.

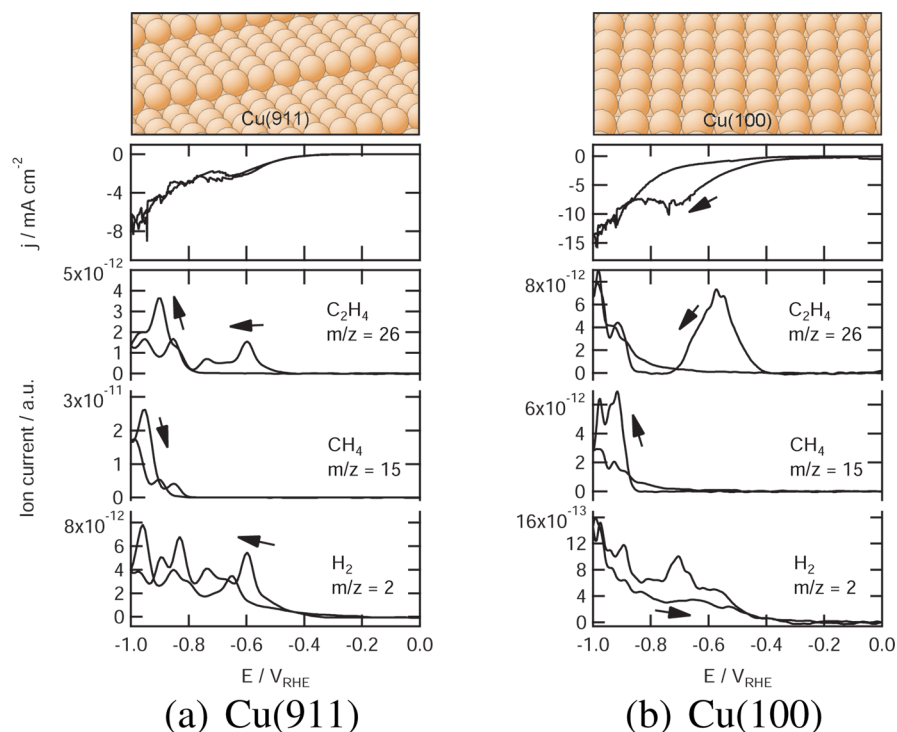


**Figure 2.** The reduction of CO in a saturated ( $\sim 1$  mM) phosphate buffer (pH 7) on (a) Cu(911) and (b) Cu(100). The top panels show the crystal facets; the middle panels, the corresponding cyclic voltammograms; and the bottom panels, the associated mass fragments of volatile products measured with OLEMS.

5.0) bubbling was used to deaerate the electrolyte before saturation of the electrolyte with carbon monoxide (Linde, 4.7).

**2.2. Online Mass Spectrometry.** Online electrochemical mass spectrometry (OLEMS) was used to detect the gaseous products formed during the reaction. The reaction products at

the electrode interface were collected with a small tip positioned close ( $\sim 10$   $\mu$ m) to the electrode.<sup>10</sup> The tip is a 0.5-mm-diameter porous Teflon cylinder with an average pore size of 10–14  $\mu$ m in a Kel-F holder. This tip is connected to a mass spectrometer with a PEEK capillary. The tip config-

urations were cleaned in a solution of 0.2 M  $K_2Cr_2O_7$  in 2 M  $H_2SO_4$  and rinsed with ultrapure water before use. A SEM voltage of 2400 V was used, except for hydrogen ( $m/z = 2$ ), for which a SEM voltage of 1200 V was used. The products were measured while changing the potential of the electrode from 0.0 to  $-1.0$  V and back at  $1\text{ mV s}^{-1}$ . Because the equilibration of the pressure in the system after introduction of the tip in the electrolyte takes a very long time, all mass fragments show a small decay during the measurement. We corrected for this background by fitting a double exponential function to the data in the potential regions where no change in activity is observed and subtracted this fit from the data. All mass fragments shown in this paper have been background-corrected in this way.

### 3. RESULTS AND DISCUSSION

**3.1. CO Reduction on Stepped Surfaces.** Figure 1 compares the reduction of carbon monoxide on Cu(322) to that on Cu(111) in a phosphate buffer of pH 7. The potential is changed from 0 to  $-1$  V and back at  $1\text{ mV s}^{-1}$ . The recorded currents are shown in the middle panel, and the volatile products measured during this potential scan are shown in the bottom panel. At  $-0.4$  V, the current increases due to the formation of hydrogen. Overall, the current is determined mainly by hydrogen evolution and does not give any specific information about the CO reduction. The hydrogen evolution leads to the formation of gas bubbles trapped between the tip and the single crystal electrode. This explains the somewhat noisy character of the observed mass signals. At  $-0.9$  V, the formation of methane and ethylene is detected, represented by  $m/z = 15$  and 26, respectively. Their formation increases when scanning to  $-1$  V and continue being formed until  $-0.7$  V in the positive going scan. The similar potential dependence for methane and ethylene is comparable to the results obtained for CO reduction on Cu(111). This indicates that methane and ethylene are being formed on the (111) terraces of the Cu(322) surfaces and that the (100) steps have no particular reactivity for CO. When comparing the ratio of  $C_2H_4/CH_4$  formation, we observe a higher ratio on Cu(322). This shift in selectivity toward  $C_2H_4$  on stepped (111) surfaces has also been observed by Hori et al.<sup>4</sup>

Figure 2 shows the results of the same experiment performed on a Cu(911) electrode, as compared with Cu(100). On this electrode, the selective formation of ethylene is observed between  $-0.5$  and  $-0.8$  V, whereas methane is not observed at these potentials. At more negative potentials, methane and ethylene are formed simultaneously. These results are very similar to CO reduction on Cu(100), indicating that also on a stepped (100) surface, the reduction of CO to ethylene occurs via two different pathways. Moreover, only (100) terraces appear to be active toward the selective ethylene formation at low overpotentials. If (100) step sites were the active sites in this process, we would expect to observe selective ethylene formation at lower potentials also on Cu(322), but from Figure 1, it is clear that this is not the case. The ratio of  $C_2H_4/CH_4$  has significantly decreased on Cu(911) compared with Cu(100). Hori et al. observed a higher selectivity toward  $C_2H_4$  formation upon the introduction of steps into Cu(100).<sup>4</sup> This selectivity change toward ethylene formation strongly depends on the terrace width: according to Hori et al., it shows an optimum at Cu(711), which has 4-atom-wide (100) terraces and a (111) step, but at 2-atom-wide terraces, the methane formation is higher and the  $C_2H_4/CH_4$  ratio lower compared with Cu(100). The presence of these narrow (100) terraces on our surface

could explain the high methane formation observed on Cu(911) in Figure 2, but this clearly would require a more detailed characterization of the surface structure. It should also be noticed that our measurements probe the selectivity during potentiodynamic cyclic voltammetry experiments, whereas Hori's experiments were based on long-term electrolysis experiments at a single potential.

Our work confirms the results of Hori et al., who showed that ethylene formation is favored on (100) facets. Gattrell et al. proposed in their review on  $CO_2$  reduction on copper electrodes that the square orientation of the atoms on the (100) terrace stabilizes the CO dimer, since it allows for the coordination of the oxygen to the surface.<sup>8</sup> Recent DFT calculations performed in our research group confirm the stabilization of the CO dimer by Cu(100), although in an orientation that is different from that proposed by Gattrell et al. The geometry of this dimer is shown in Figure 3a.<sup>13</sup> These DFT results show that the CO dimer is adsorbed on two opposing bridge sites, binding through one O atom and one C atom to four Cu atoms.

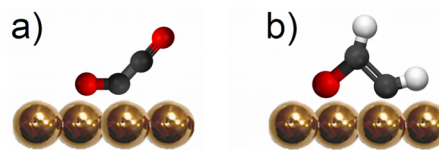


**Figure 3.** Key intermediates in the formation of ethylene: (a) the CO dimer and (b) the oxametallacycle.

It has been observed that many electrocatalytic reactions that involve the breaking or making of C–O, N–O, N–N, and C–C bonds, such as ammonia oxidation, dimethylether oxidation, and nitrite reduction, prefer the (100) site geometry.<sup>14</sup> It is assumed that in such a geometry, the repulsion between two fragments occupying two opposing bridge sites is minimal because sharing of metal atoms can be avoided. It seems that this also applies for the reduction of CO so that the square arrangement of the atoms stabilizes the reaction step/intermediates in which the C–C bond is formed.

Steps in (100) facets are usually unbeneficial for the aforementioned bond-breaking/-making reactions;<sup>14</sup> however, according to Hori et al., the formation of ethylene is enhanced by the presence of (111) and (110) steps in the (100) surface, with an optimum at Cu(711), which has 4-atom-wide (100) terraces and a (111) step.<sup>4</sup> Terraces smaller than 4 atoms probably lower the possible assemblies of surface sites where the CO dimer can be formed, thereby limiting the C–C bond formation.

**3.2. Ethylene Oxide Reduction.** In a recent paper, we showed that the only  $C_2$  species that can be reduced to ethylene on (polycrystalline) copper electrodes is ethylene oxide.<sup>15</sup> Therefore, we have proposed an oxametallacycle (Figure 3b) as an intermediate in the formation of ethylene. The aforementioned DFT calculations on Cu(100) also suggest an oxametallacycle as an intermediate in the lowest energy pathway from CO to ethylene.<sup>13</sup> To investigate whether the formation of this oxametallacycle is surface-structure-dependent, we have performed the reduction of ethylene oxide on Cu(111) and Cu(100). From Figure 4, it can be seen that there is a clear potential difference in the formation of ethylene on Cu(111) and Cu(100). Ethylene is formed at  $-0.3$  V on Cu(100), whereas it is formed at  $-0.6$  V on Cu(111), and

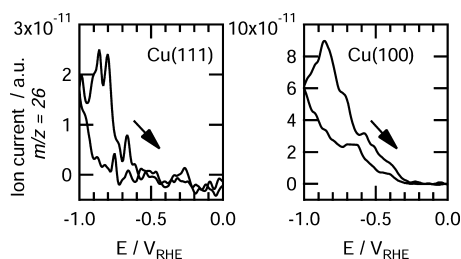


**Figure 4.** The reduction of ethylene oxide to ethylene on Cu(111) (left) and Cu(100) (right).

although our OLEMS data do not give direct quantitative information about the amounts of product formed, we can still conclude that there is more ethylene formed on Cu(100) compared with Cu(111). Therefore, the stabilization of the oxametallacycle on Cu(100) is in agreement with our model of why ethylene formation is enhanced on this surface.

**3.3. CO Reduction on Cu(110).** To investigate the reactivity of (110) sites, we have also investigated the reduction of CO on Cu(110), the results of which are shown in Figure 5.

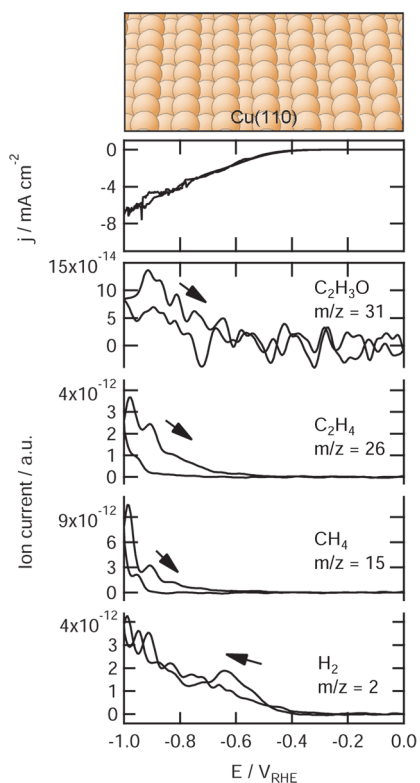


**Figure 5.** Top: the Cu(110) crystal facet. Middle: cyclic voltammogram for the reduction of a CO saturated ( $\sim 1$  mM) phosphate buffer (pH 7) on Cu(110). Bottom: associated mass fragments of volatile products measured with OLEMS.

The formation of both methane and ethylene starts at  $\sim -0.9$  V and continues until  $-0.6$  V in the positive-going scan, similar to the results obtained for Cu(111). Since (110) could also be written as  $[2(111) \times (111)]$  and therefore exhibits only (111) sites, this could explain the similar potential dependence as observed on Cu(111). Methane and ethylene exhibit the same potential dependence, suggesting a common reaction intermediate, as observed on Cu(322) and Cu(111). Hori et al. observed that on surfaces with (110) terraces, relatively high

amounts of acetaldehyde, ethanol, propanol, and other  $C_2$  and  $C_3$  species are formed.<sup>4</sup> We have detected traces of the mass fragment  $m/z = 31$  below  $-0.7$  V, shown in Figure 5. This fragment is characteristic for primary alcohols. We have not observed this fragment for CO reduction on Cu(100) or Cu(111).

#### 4. CONCLUSIONS

In this letter, we have shown that the selective reduction of CO to ethylene on copper electrodes at low overpotentials occurs on Cu(100) terraces, whereas (100) step sites are not involved in this reaction. The reduction of CO on Cu(110) exhibits a similar potential dependence on Cu(111), and more alcohols are observed.

#### AUTHOR INFORMATION

##### Corresponding Author

\*E-mail: m.koper@chem.leidenuniv.nl.

##### Notes

The authors declare no competing financial interest.

#### ACKNOWLEDGMENTS

This work was supported financially by the (Dutch) National Research School Combination–Catalysis (NRSC-C).

#### REFERENCES

- Gattrell, M.; Gupta, N.; Co, A. *Energy Convers. Manage.* **2007**, *48*, 1255–1265.
- Hori, Y. In *Modern Aspects of Electrochemistry*; Vayenas, C. G., White, R. E., Gamboa-Aldeco, M. E., Eds.; Springer: New York, 2008; Vol. 42.
- Hori, Y.; Kikuchi, K.; Suzuki, S. *Chem. Lett.* **1985**, 1695–1698.
- Hori, Y.; Takahashi, I.; Koga, O.; Hoshi, N. *J. Mol. Catal. A: Chem.* **2003**, *199*, 39–47.
- Schouten, K. J. P.; Qin, Z.; Pérez Gallent, E.; Koper, M. T. M. *J. Am. Chem. Soc.* **2012**, *134*, 9864–9867.
- Durand, W. J.; Peterson, A. A.; Studt, F.; Abild-Pedersen, F.; Nørskov, J. K. *Surf. Sci.* **2011**, *605*, 1354–1359.
- Hori, Y.; Takahashi, R.; Yoshinami, Y.; Murata, A. *J. Phys. Chem. B* **1997**, *101*, 7075–7081.
- Gattrell, M.; Gupta, N.; Co, A. *J. Electroanal. Chem.* **2006**, *594*, 1–19.
- Hori, Y.; Wakebe, H.; Tsukamoto, T.; Koga, O. *Surf. Sci.* **1995**, *335*, 258–263.
- Wonders, A. H.; Housmans, T. H. M.; Rosca, V.; Koper, M. T. M. *J. Appl. Electrochem.* **2006**, *36*, 1215–1221.
- Magnussen, O. M.; Zitzler, L.; Gleich, B.; Vogt, M. R.; Behm, R. *J. Electrochim. Acta* **2001**, *46*, 3725–3733.
- Schouten, K. J. P.; Pérez Gallent, E.; Koper, M. T. M. *J. Electroanal. Chem.* **2013**, *699*, 6–9.
- Calle-Vallejo, F.; Koper, M. T. M. *Angew. Chem., Int. Ed.* **2013**, in press.
- Koper, M. T. M. *Nanoscale* **2011**, *3*, 2054–2073.
- Schouten, K. J. P.; Kwon, Y.; van der Ham, C. J. M.; Qin, Z.; Koper, M. T. M. *Chem. Sci.* **2011**, *2*, 1902–1909.